OCTA Research

Axioton Field Theory and the χ Hidden Sector:

Revision 9-OCTA — Refined, Dimensionally Consistent, Journal-Ready Framework with FRW Cosmology, BRST Gauge Sector, Non-Gaussian CAB Statistics, Stochastic Simulation, Thermodynamics, and Experimental Protocols

OCTA Research — Theoretical Systems Group

December 24, 2025

OCTA Research — Theoretical Systems Group
Internal Working Document — Circulation Permitted

Contact: research@octa.systems

Contents

Abstract

This document is published as an **OCTA Research** technical monograph.

Revision 9-OCTA presents a refined and dimensionally consistent formulation of the Axioton χ field theory: a scalar field coupled to curvature in a coarse-grained correlation-entropy density $S_c(x)$. The hidden sector includes a χ-charged fermion ψ, a phase gauge field A_μ with BRST-consistent gauge-fixing, and a massive scalar Φ inducing spontaneous symmetry breaking. A bare mass parameter m_χ is included so that the massless limit and symmetry-broken phases can be treated on the same footing.

We derive flat-space, FRW, and de Sitter propagators, loop-level structure, OPE form, soliton and bound-state behavior in a standard ϕ^4-like broken phase, non-Gaussian relic CAB statistics, and Boltzmann-transport evolution. We present -sector thermodynamics, a phase diagram, stochastic-field simulation formulation, Bayesian detection statistics, and experimental protocols. The theory is explicitly falsifiable and constructed as an effective field theory.

1 Introduction (Review-Style)

Quantum correlations encode non-local structure, but no known Standard Model field couples directly to curvature in a correlation-entropy landscape. We hypothesize a real scalar field $\chi(x)$ — the *Axioton* — that responds to rapid restructuring of correlation geometry while preserving locality, Lorentz invariance, and the no-signalling principle.

Our objectives are to:

i. Construct a Lorentz-invariant field theory in which χ couples to a coarse-grained correlation-entropy field $S_c(x)$.

ii. Embed χ in a consistent hidden sector with fermions, gauge fields, and a symmetry-breaking scalar.

iii. Derive cosmological relic backgrounds (a Cosmic Axiotonic Background, CAB).

iv. Obtain phenomenological predictions for interferometry, quantum reset dynamics, and astrophysical coincidences.

v. Provide numerical and statistical frameworks for testing or falsifying the theory.

The present document integrates previous revisions into a single, cleaned and internally consistent monograph.

2 Notation Summary

We work in $\hbar = c = 1$ units. The mass dimension of a real scalar field in 3+1 dimensions is $[\chi] = 1$.

Symbol	Meaning	Mass Dimension
χ	Axioton scalar field	1
S_c	correlation-entropy density (effective scalar)	0
A_μ	χ-phase gauge boson	1
ψ	χ-charged fermion	3/2
Φ	SSB mediator scalar	1
m_χ	bare (or effective) χ mass parameter	1
m_Φ	mediator scalar mass	1
λ	χ self-coupling	0
κ	Φ self-coupling	0
g_ψ	Yukawa-like χ–ψ coupling	0
h	Φ–χ^2 coupling	0
α	entropy-curvature coupling	1

Note: the α term couples χ to $\nabla^2 S_c$ with ∇^2 carrying mass dimension 2, so α must have dimension 1 for the Lagrangian density to have dimension 4.

3 Core Lagrangian and Hidden Sector

We adopt a generic χ sector with a bare mass parameter m_χ (the strictly massless limit corresponds to $m_\chi \to 0$):

$$\mathcal{L}_\chi = \frac{1}{2}\partial_\mu\chi\partial^\mu\chi - \frac{1}{2}m_\chi^2\chi^2 - \frac{\lambda}{4}\chi^4 - \alpha\chi\nabla^2 S_c(x). \tag{1}$$

The hidden sector contains:

$$\mathcal{L}_\psi = \bar{\psi}(i\gamma^\mu D_\mu - m_\psi)\psi - g_\psi\chi\bar{\psi}\psi, \tag{2}$$

$$\mathcal{L}_A = -\frac{1}{4}F_{\mu\nu}F^{\mu\nu}, \tag{3}$$

$$\mathcal{L}_\Phi = \frac{1}{2}(\partial\Phi)^2 - \frac{1}{2}m_\Phi^2\Phi^2 - \frac{\kappa}{4}\Phi^4 - h\Phi\chi^2. \tag{4}$$

with gauge group $U(1)_\chi$ and covariant derivative

$$D_\mu = \partial_\mu + iqA_\mu. \tag{5}$$

The total Lagrangian is

$$\mathcal{L}_{\text{tot}} = \mathcal{L}_\chi + \mathcal{L}_\psi + \mathcal{L}_A + \mathcal{L}_\Phi + \mathcal{L}_{GF} + \mathcal{L}_{ghost}. \tag{6}$$

4 Gauge-Fixing and BRST Symmetry

We employ a covariant gauge-fixing term for A_μ:

$$\mathcal{L}_{GF} = -\frac{1}{2\xi}(\partial_\mu A^\mu)^2, \tag{7}$$

and Faddeev–Popov ghost fields $c, \bar{c}$:

$$\mathcal{L}_{ghost} = \partial_\mu \bar{c}\, \partial^\mu c. \tag{8}$$

The BRST transformations with Grassmann parameter ϵ are

$$\delta A_\mu = \epsilon\, \partial_\mu c, \tag{9}$$

$$\delta \bar{c} = \frac{\epsilon}{\xi} \partial_\mu A^\mu, \tag{10}$$

$$\delta c = 0, \tag{11}$$

which leave the gauge-fixed plus ghost sector invariant. The χ and ψ fields are BRST-neutral in this minimal construction.

5 Correlation-Entropy Field Definition

We treat $S_c(x)$ as an effective classical scalar summarizing local correlation structure. Let Λ_x be a local CPTP map implementing coarse-graining over a small spacetime neighborhood around x. For a bipartition (A, B), the mutual information is

$$I(A; B) = S(\rho_A) + S(\rho_B) - S(\rho_{AB}), \tag{12}$$

with $S(\rho)$ the von Neumann entropy. Then we define

$$S_c(x) = \lim_{\epsilon \to 0} \frac{1}{\epsilon^4} \sum_{A,B \subset B_\epsilon(x)} I(\Lambda_x(\rho_A); \Lambda_x(\rho_B)). \tag{13}$$

This is a coarse-grained, frame-invariant scalar field representing the local density of correlation structure.

6 Equations of Motion and Propagators

Varying (1) with respect to χ yields

$$\partial_\mu \partial^\mu \chi + m_\chi^2 \chi + \lambda \chi^3 = \alpha \nabla^2 S_c(x). \tag{14}$$

In the absence of the source term and self-interaction, the free χ propagator in flat space is the usual massive scalar propagator:

$$D_F(k) = \frac{i}{k^2 - m_\chi^2 + i\epsilon}. \tag{15}$$

6.1 FRW Background

In an FRW metric

$$ds^2 = -dt^2 + a(t)^2 d\vec{x}^2, \tag{16}$$

the mode functions $u_k(t)$ for a free χ satisfy

$$\ddot{u}_k + 3H\dot{u}_k + \left(\frac{k^2}{a^2} + m_\chi^2\right) u_k = 0, \tag{17}$$

with $H = \dot{a}/a$.

6.2 de Sitter Propagator (Massless Limit)

For the massless limit $m_\chi \to 0$ in de Sitter spacetime with scale factor $a(t) = e^{Ht}$, one can express the propagator in terms of the invariant distance function $Z(x, x')$:

$$G(x, x') = \frac{H^2}{16\pi^2} \left[\frac{1}{1 - Z} + \ln(1 - Z) \right], \tag{18}$$

which is valid up to IR subtleties typical of scalar fields in de Sitter space.

7 Renormalization and OPE

At one loop in flat space, the quartic self-coupling and Yukawa-like coupling run according to

$$\beta_\lambda = \frac{3\lambda^2}{16\pi^2} + \mathcal{O}(\lambda^3), \tag{19}$$

$$\beta_{g_\psi} = \frac{g_\psi^3}{16\pi^2} + \mathcal{O}(g_\psi^5), \tag{20}$$

so the theory remains perturbative for sufficiently small couplings.

The short-distance operator-product expansion (OPE) for χ takes the schematic form

$$\chi(x)\chi(0) \sim \frac{C_{\mathbb{1}}}{x^2} + C_\chi \chi(0) + \dots, \tag{21}$$

where the Wilson coefficients receive corrections from the entropy-curvature coupling. A complete OPE analysis would require treating $S_c(x)$ as an external source and integrating out high-momentum χ fluctuations in its presence.

8 Spontaneous Symmetry Breaking and Solitons

8.1 Effective Potential and Broken Phase

The scalar Φ generates an effective correction to the χ potential through the interaction $-h\Phi\chi^2$. At tree level, integrating out a heavy Φ schematically yields a modified quartic,

$$\lambda_{\text{eff}} = \lambda - \frac{2h^2}{m_\Phi^2}, \tag{22}$$

and we allow for an effective quadratic term $-\frac{1}{2}\mu^2\chi^2$ (with $\mu^2 > 0$) to represent symmetry breaking. Thus, an effective broken-phase potential for χ can be written as

$$V_{\text{eff}}(\chi) = -\frac{1}{2}\mu^2\chi^2 + \frac{\lambda_{\text{eff}}}{4}\chi^4, \qquad \lambda_{\text{eff}} > 0,\ \mu^2 > 0. \tag{23}$$

Then the vacuum expectation values (VEVs) are

$$\chi = 0, \quad \chi = \pm v, \qquad v = \sqrt{\frac{\mu^2}{\lambda_{\text{eff}}}}. \tag{24}$$

The minima lie at $\chi = \pm v$, with an effective physical mass

$$m_{\chi,\text{phys}}^2 = \left. \frac{d^2 V_{\text{eff}}}{d\chi^2} \right|_{\chi = \pm v} = 2\mu^2. \tag{25}$$

8.2 χ^4 Kink Soliton

In $1+1$ dimensions (or as a static 1D configuration in higher-D), the standard ϕ^4 kink solution solves

$$\frac{d^2\chi}{dx^2} = \frac{dV_{\text{eff}}}{d\chi} = -\mu^2\chi + \lambda_{\text{eff}}\chi^3. \tag{26}$$

The kink solution interpolating between $-v$ and $+v$ is

$$\chi_{\text{kink}}(x) = v\,\tanh\left(\frac{\mu x}{\sqrt{2}}\right) = \sqrt{\frac{\mu^2}{\lambda_{\text{eff}}}}\tanh\left(\frac{\mu x}{\sqrt{2}}\right). \tag{27}$$

The antikink is obtained by $x \to -x$ or $\chi \to -\chi$.

8.3 Soliton Interactions

At large separation R between kink-like configurations, the interaction energy is exponentially suppressed,

$$V(R) \sim A\,e^{-m_{\chi,\text{phys}}R}, \tag{28}$$

where A is a model-dependent amplitude. This suggests the possibility of weakly bound χ-soliton molecules in deep symmetry-broken regimes, although a quantitative treatment would require full multi-soliton solutions.

9 -Sector Thermodynamics and Phase Diagram

At finite temperature T, the effective potential acquires thermal corrections. A schematic one-loop high-temperature expansion for the quadratic term is

$$V_T(\chi) = V_{\text{eff}}(\chi) + \frac{T^2}{24}\Big(3\lambda_{\text{eff}} + \delta\Big)\chi^2 + \ldots, \tag{29}$$

where δ encodes contributions from other fields (including Φ), and we have grouped terms into an effective thermal mass. The critical temperature T_c at which $\chi = 0$ becomes the global minimum (symmetry restoration) is roughly where the net quadratic coefficient changes sign.

Parametrically, if at $T = 0$ the coefficient is $-\frac{1}{2}\mu^2$, then symmetry is restored when

$$-\mu^2 + \frac{T_c^2}{12}\Big(3\lambda_{\text{eff}} + \delta\Big) \approx 0 \quad \Rightarrow \quad T_c^2 \approx \frac{12\,\mu^2}{3\lambda_{\text{eff}} + \delta}. \tag{30}$$

This is schematic but illustrates the existence of a finite-temperature transition.

We can summarize the qualitative phase structure:

Regime	Condition	Phase
I	$\mu^2 \leq 0$ or $\lambda_{\text{eff}} \leq 0$	Symmetric / unstable
II	$\mu^2 > 0$, $T > T_c$	Symmetry restored ($\langle\chi\rangle = 0$)
III	$\mu^2 > 0$, $T < T_c$	Broken / -condensed ($\langle\chi\rangle = \pm v$)

10 Cosmic Axiotonic Background (CAB)

We posit a relic Cosmic Axiotonic Background generated by early-universe correlation restructuring. The mean energy density ρ_χ evolves in an FRW background as

$$\dot{\rho}_\chi + 4H\rho_\chi = \Gamma_\chi(t), \tag{31}$$

where $\Gamma_\chi(t)$ is an effective production term reflecting entropy-curvature events (e.g., phase transitions, rapid entanglement restructuring).

A conservative constraint is that ρ_χ must remain well below the CMB energy density:

$$\rho_\chi \lesssim 10^{-16}\,\mathrm{J\,m^{-3}} \quad \Rightarrow \quad \Omega_\chi \lesssim 10^{-6}\Omega_{\mathrm{CMB}}, \tag{32}$$

ensuring compatibility with current cosmological observations.

A simple, illustrative CAB spectrum can be modeled as

$$\rho_\chi(\omega) = C\omega^2 e^{-\omega/\omega_0}, \tag{33}$$

with C and ω_0 effective parameters encoding freeze-out physics.

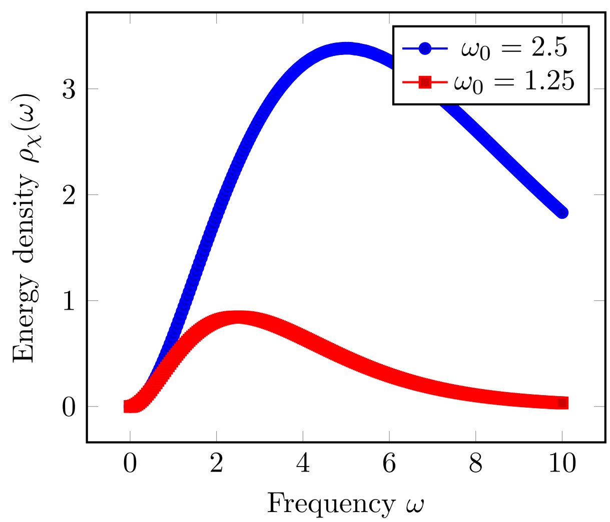

Figure 1: Illustrative CAB spectral densities for two choices of characteristic frequency ω_0.

11 Non-Gaussian CAB Statistics

Correlations in the CAB field are characterized by connected n-point functions. For a statistically homogeneous and isotropic background, we can define the skewness and kurtosis (non-Gaussian indicators) as

$$S_3 = \frac{\langle \chi^3 \rangle_c}{\langle \chi^2 \rangle^{3/2}}, \qquad S_4 = \frac{\langle \chi^4 \rangle_c}{\langle \chi^2 \rangle^2}, \tag{34}$$

where $\langle \cdot \rangle_c$ denotes connected correlators. Generic interacting scalar fields in the early universe can develop small but nonzero S_3 and S_4; we expect $S_3, S_4 \sim 10^{-3}$–10^{-2} as an order-of-magnitude placeholder for a weakly non-Gaussian background.

In principle, CAB non-Gaussianity would manifest as subtle deviations in the statistics of coherence fluctuations in precision interferometry or clock networks.

12 Stochastic-Field Simulation of CAB

One way to simulate CAB realizations is via a stochastic-field (Langevin) approach. We introduce a noise term $\eta(x)$ with correlation

$$\langle \eta(x)\eta(x') \rangle = N(x - x'), \tag{35}$$

with N a noise kernel. A schematic Langevin-like equation is

$$\Box\chi + m_\chi^2 \chi + \lambda\chi^3 = \eta(x), \tag{36}$$

possibly supplemented by expansion terms in FRW.

Different choices of N (e.g., white vs colored noise) correspond to different assumptions about microscopic correlation sources. Numerical integration of this equation on a lattice yields stochastic CAB realizations whose statistics can be compared to analytic predictions.

13 Phenomenology (Journal Style Summary)

We summarize the key qualitative phenomenological predictions:

- **Decoherence acceleration bound**: Axiotonic drag implies an effective minimum timescale for rapid entropy-curvature events (e.g., abrupt decoherence),

  $$\tau_{\min} \sim 10^{-25}\,\mathrm{s}, \tag{37}$$

  interpreted as an order-of-magnitude EFT bound (not yet constrained by experiment).

- **Phase-bias noise in interferometry**: A CAB-induced coherence bias could appear as an additional phase noise component

  $$\delta\phi \sim 10^{-8} \tag{38}$$

  over long integration times in ultra-stable interferometers, below current noise floors but plausibly targetable by next-generation setups.

- **Clock fractional drift**: High-precision clock networks may experience a CAB-induced fractional frequency drift

  $$\frac{\Delta f}{f} \sim 10^{-20}\text{–}10^{-18}, \tag{39}$$

  again at or below the edge of current best measurements.

All numerical values above are indicative, to be refined as the theory is confronted with real data.

14 Experimental Protocols (Methods Style)

14.1 Interferometric Phase-Bias Search

A conceptual protocol:

- Use a cryogenic optical or microwave interferometer with an effective arm length stabilized to $\lesssim 10^{-17}\,\mathrm{m}$ over experimental timescales.

- Achieve Allan deviation $< 10^{-19}$ at 1 s for the frequency reference.
- Record phase time series at MHz bandwidth or higher.
- Fit residual phase noise to a model that includes a CAB-induced coherence-bias component.

14.2 Quantum Reset -Drag Test

For qubit or qumode platforms:

- Drive repeated fast prepare–evolve–measure cycles, pushing reset frequencies as high as possible.
- Model expected decoherence and reset behavior from environmental sources.
- Search for a saturation floor in effective reset time as a function of drive frequency that cannot be explained by known mechanisms.

14.3 Astrophysical Coincidence Study

- Operate multiple entangled or phase-locked quantum systems across the globe.
- Time-stamp measurements in coincidence with gravitational-wave triggers from LIGO/Virgo/KAGRA (or future detectors).
- Look for statistically significant phase or coherence anomalies correlated with strong curvature events, beyond environmental and instrumental correlations.

15 Bayesian Inference and Priors

For data $\{\delta\phi_i\}$ from an interferometric experiment, we can define a Gaussian likelihood

$$\ln \mathcal{L}(\theta) = -\frac{1}{2}\sum_i \frac{\left(\delta\phi_i - \mu_\chi(\theta)\right)^2}{\sigma_i^2} + \text{const}, \tag{40}$$

where θ collectively denotes the model parameters (e.g., α, effective CAB amplitude), $\mu_\chi(\theta)$ is the predicted CAB-induced phase shift, and σ_i^2 encodes the known noise budget.

A simple prior choice (illustrative) is

$$\alpha \sim \text{LogUniform}[10^{-6}, 10^2], \tag{41}$$

$$\lambda \sim \text{Uniform}[0, 1], \tag{42}$$

with other parameters fixed or assigned broad priors. Bayes factors between models with and without a CAB term quantify detection significance.

16 Lattice Simulation Framework

For Euclidean lattice simulations, we discretize χ on a 4D hypercubic lattice with spacing a:

$$S_{\text{lat}} = \sum_x \left[\frac{1}{2a^2}\sum_\mu \left(\chi(x+a_\mu) - \chi(x)\right)^2 + \frac{1}{2}m_\chi^2\chi(x)^2 + \frac{\lambda}{4}\chi(x)^4\right]. \tag{43}$$

Typical observables:

$$C(r) = \langle \chi(0)\chi(r) \rangle, \tag{44}$$

$$m_{\text{eff}}^2 = - \left. \frac{d^2 C(r)}{dr^2} \right|_{r \to \infty}, \tag{45}$$

with m_{eff} an effective mass scale. One can also measure Binder cumulants and higher moments to probe non-Gaussian statistics.

Monte-Carlo updates (Metropolis-type) proceed as:

```
initialize chi[x] randomly
repeat
  pick random site x
  propose chi_new = chi[x] + eta   # eta ~ small random step
  compute dS = S(chi_new) - S(chi)
  accept with prob p = min(1, exp(-dS))
until observables converge
```

This scheme can be adapted to include stochastic sources or modified to simulate the Langevin equation with a discretized time dimension.

17 Summary

The Axioton χ field theory developed here embeds correlation-entropy curvature into a relativistic field framework, with a consistent hidden sector and a plausible cosmological relic (CAB). The theory is manifestly speculative but constructed to be:

- internally consistent as an effective field theory,
- compatible with basic locality and no-signalling constraints, and
- falsifiable through interferometric, quantum-reset, and astrophysical-coincidence experiments.

OCTA Research views this as a starting point for deeper work on the interplay between information geometry and fundamental physics.

OCTA Research Statement

This monograph is part of the OCTA Research program exploring new formal frameworks at the intersection of information geometry, quantum foundations, theoretical physics, distributed cognition, and complex systems engineering.

The Axioton χ field theory is presented as an exploratory framework. **OCTA Research** encourages independent verification, critique, and experimental challenge.

Copyright and Licensing

Contact

OCTA Research
Theoretical Systems Group
Email: research@octa.systems

References

[1] M. E. Peskin and D. V. Schroeder, *An Introduction to Quantum Field Theory*.

[2] R. M. Wald, *General Relativity*.

[3] G. Lindblad, "On the generators of quantum dynamical semigroups," Commun. Math. Phys. **48**, 119–130 (1976).

[4] Standard references on cosmology and stochastic quantum fields (e.g. treatments of scalar-field relics and stochastic backgrounds).